Bridging evolutionary game theory and metabolic models for predicting microbial metabolic interactions

Jingyi Cai [1], Tianwei Tan[1*], Siu Hung Joshua Chan[2**],

1 National R&D Center for Biorefinery, Beijing University of Chemical Technology, Beijing 100029, China

2 Department of Chemical and Biological Engineering, Colorado State University, Fort Collins, CO 80523, USA

*Tianwei Tan: twtan@mail.buct.edu.cn ** Siu Hung Joshua Chan: Joshua.Chan@colostate.edu,

Abstract

Microbial metabolic interactions impact ecosystems, human health and biotechnological processes profoundly. However, their determination remains elusive, invoking an urgent need for predictive models that seamlessly integrate ecological, evolutionary principles and metabolic details. Recognizing that metabolic interactions form a complex game in which an individuals strategies are a metabolic flux space constrained also by other individuals strategies, we formulated a bi-level optimization framework termed NECom, which is free of a long hidden 'forced altruism' setup adopted by previous algorithms, for prediction of Nash equilibria of microbial metabolic interactions with significantly enhanced accuracy. A complementary shadow-price-based iterative algorithm was used to predict state transitions and draw analogy to traditional payoff matrix analysis. We successfully predicted several classical games in the context of metabolic interactions that were falsely or incompletely predicted by existing methods, including prisoner's dilemma, snowdrift and mutualism, providing insights into why mutualism is favorable despite seemingly costly cross-feeding metabolites, and demonstrating NECom's potential to predict heterogeneous phenotypes among the same species. An in-depth analysis on a reported algae-yeast co-culture showed that NECom can capture and explain experimental trends using a minimal amount of experimental data as inputs without ad-hoc parameters, and that growth limiting crossfeeding metabolites can be pinpointed by shadow price analysis of NECom solutions to explain frequency-dependent growth pattern, shedding light on control of microbial populations.

Introduction

In nature, microorganisms seldom exist in isolate. Instead, they form communities governed by different types of interactions, which play essential roles in adaptation to environment [1–3] and evolution of species [4–8]. Beside the theoretical importance, microbial interactions are also key to applications ranging from drug precursor synthesis [9, 10] to remediation of the gut microbiome [11–14], from degradation of cellulose for biorefinery [15–17] to microbial power generation [18]. Among microbial interactions, exchange of metabolites is especially important and arguably responsible for the fact that more than 99% of bacterial species are not cultivable [3, 19, 20]. Understanding metabolic interactions is a fundamental task in microbiome science. Despite continual progresses in determining metabolite exchanges using experimental approach such as spatially separated apparatus designs [21, 22], isotope probing [23, 24] and tracing [25] techniques, 16s RNA analysis [26] and metabolome analysis [27], we still need governing principles to predict and understand these metabolic interactions.

Benefiting from the advancement of genome-scale metabolic models [28], methods of extending constraint-based modeling to microbial communities have been proposed since a decade ago [29] while new challenges emerged in the process. Joint flux balance analysis (Joint-FBA) was first introduced to model a microbial community as a 'super' organism containing the compartments for each organism and an additional compartment for inter-cellular metabolite exchange [29, 30]. The total community biomass was maximized to predict metabolism. Methods based on Joint-FBA for analyzing host-microbe and microbe-microbe interactions were widely applied to the gut microbiome [31–34]. Later FBA was adapted for dynamic modeling of microbial co-culture [35, 36]. Succeeding efforts include regularization of the optimization problem in each time step to ensure a well-conditioned dynamical system [37] and incorporation of spatiotemporal elements [38–42]. In order to reconcile the community and individual objective functions, OptCom, a bilevel optimization algorithm was developed to optimize the individual fitness in the inner problem, while optimizing the community fitness in the outer problem [43]. To address the effect of viable abundance on the inter-cellular fluxes at population steady state, community FBA (cFBA) [44] generalized joint-FBA by adding parameterized abundances as weights to exchange fluxes. SteadyCom [45] as a reformulation of cFBA enabled efficient computation for flux variability analysis and other constraint based modeling techniques for communities with a large number of organisms. Recently, there have been efforts to simulate communities with a large number of species [46, 47] or handle a large quantity of cases [48–50]. Joint-FBA and its linear derivatives are usually employed to avoid intractable computation. However, in most static FBA-based algorithms, some constraints and the community objective function might force individual organisms to produce a certain amount of metabolites for other members prior to optimizing its own fitness whenever doing so the community-level

objective function is optimal. Here we call this 'forced altruism'. We believe that forced altruism is potentially applicable to microbes that are physically connected, e.g., by nanotubes [51, 52] or to endosymbiosis, since inter-cellular exchange under these situations are likely governed by concentration gradients or regulation by the host, respectively. In general for microbes in a co-culture separate from each other by cell envelopes and not controlled by higher-level regulatory mechanisms (e.g., host-regulation, quorum sensing etc), however, the applicability of 'forced altruism' constraints should be questioned because microbial cells with higher individual fitness are likely to be favored by natural selection.

Consequently, as a necessary condition for evolutionary stability, true Nash equilibria (NE) in community metabolic networks should be the targets to identify, in which each microbe maximizes its fitness function in the given environment. In the context of community metabolic networks, the microbial game is significantly different from those studied previously which treat a single microbial cell as the basic unit with ad-hoc metabolic details [53–59]. Instead, in community metabolic networks, each microbe is represented as the sum of its constituent biomacromolecules synthesized from the network. The available strategies for each player are any possible flux distributions (the entire set of reaction fluxes) satisfying biochemical principles and constrained by substrate availability, which depends not only on the nutrients in the environment but also the strategies of other players in terms of the cross-feeding metabolites they may produce [60]. The metabolic details, continuous flux space and interdependence of available strategies between players characterize a unique class of microbial games in community metabolic networks (fig. 1) which require novel game-theoretical methods. In this paper we firstly introduce a method termed 'FShap' to construct payoff matrices or more generally state transition maps of interacting species with the solution of FBA [61], so that the Nash equilibrium can be deduced in a similar fashion to traditional payoff matrix analysis. Then we introduce a bi-level mixed integer optimization framework free of forced altruism termed NECom. We demonstrate the ability of the proposed algorithms to identify Nash equilibrium (NE) in toy community metabolic models that are analogous to classical games and predict reasonable interactions not captured by joint FBA and OptCom. We further validate NECom by analyzing a previously reported algae-yeast co-culture where NECom is able to predict important trends observed from the experimental data with minimal input from the data and to provide insights into the metabolic states of the two organisms.

Result and Discussion

Microbial metabolic games and cross-feeding metabolites

Distinguished from most traditional games, a microbial community is a dynamic system in which each microbe has its cross-feeding profile (strategy) subject to transition from one state to another depending on the profile of other microbes (fig. 1). Under natural selection, new states might keep emerging before the system reaches an evolutionary stable state (ESS) which is a Nash equilibrium (a state where unilateral change of strategies by any player cannot bring fitness gain) not invadable by alternative strategies.

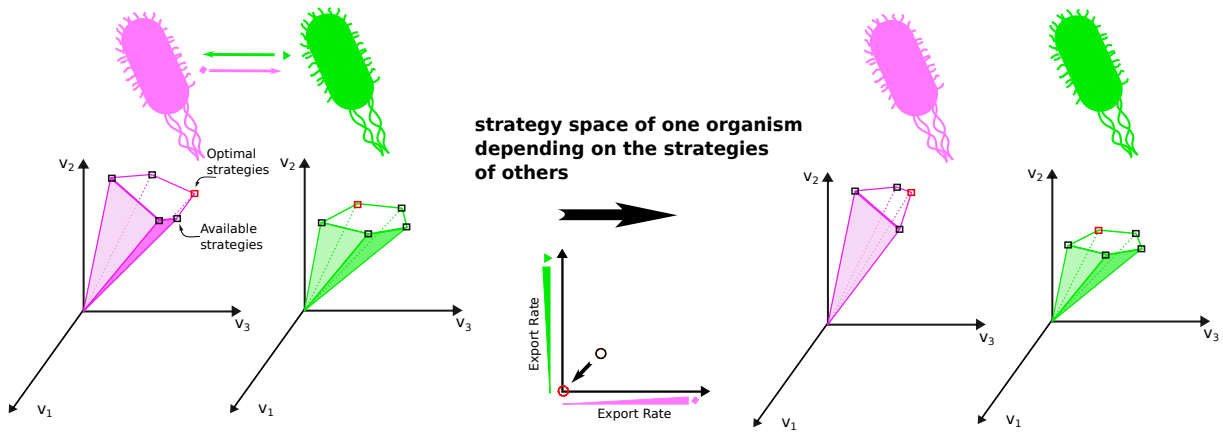

Figure 1. Schematic diagram to illustrate the interactive strategy space in metabolic games Strategy space of one organism can be shaped by the other organism's strategies during metabolic interaction, since an available strategy for an organism is any feasible flux distribution satisfying the pseudo-steady-state condition and reaction directionality constrained by the availability of extracellular metabolites, which can be affected by other community members. Interactive strategy space causes the complexity of microbial metabolic games, distinguishing microbial metabolic game from most traditional games.

State transition is governed by 'payoffs', i.e., the total impacts of strategies on each member at a starting reference state. In a two-member system, the relative payoffs associated to combinations of strategies chosen by each member are computed, placed orderly in so-called 'payoff matrices' (for examples, see fig. 2e-g), before compared to find Nash equilibria. Then, transition to the next state(s) can be determined.

Based on the aforementioned logic we develop a novel method to update metabolic cross-feeding states for interacting microbes (fig. 2a). In this method, the payoff of a single strategy on a community member is considered as fitness gain due to metabolite uptake or fitness decrease due to metabolite export. Therefore, the relative payoff in transiting to another state from the current can be quantified by the shadow price of the lower bound constraint of metabolite exchange reactions in a FBA solution. We termed the method FBA Shadow price based Payoffs (FShaP). Payoff matrices then can be constructed and the next state(s) can be

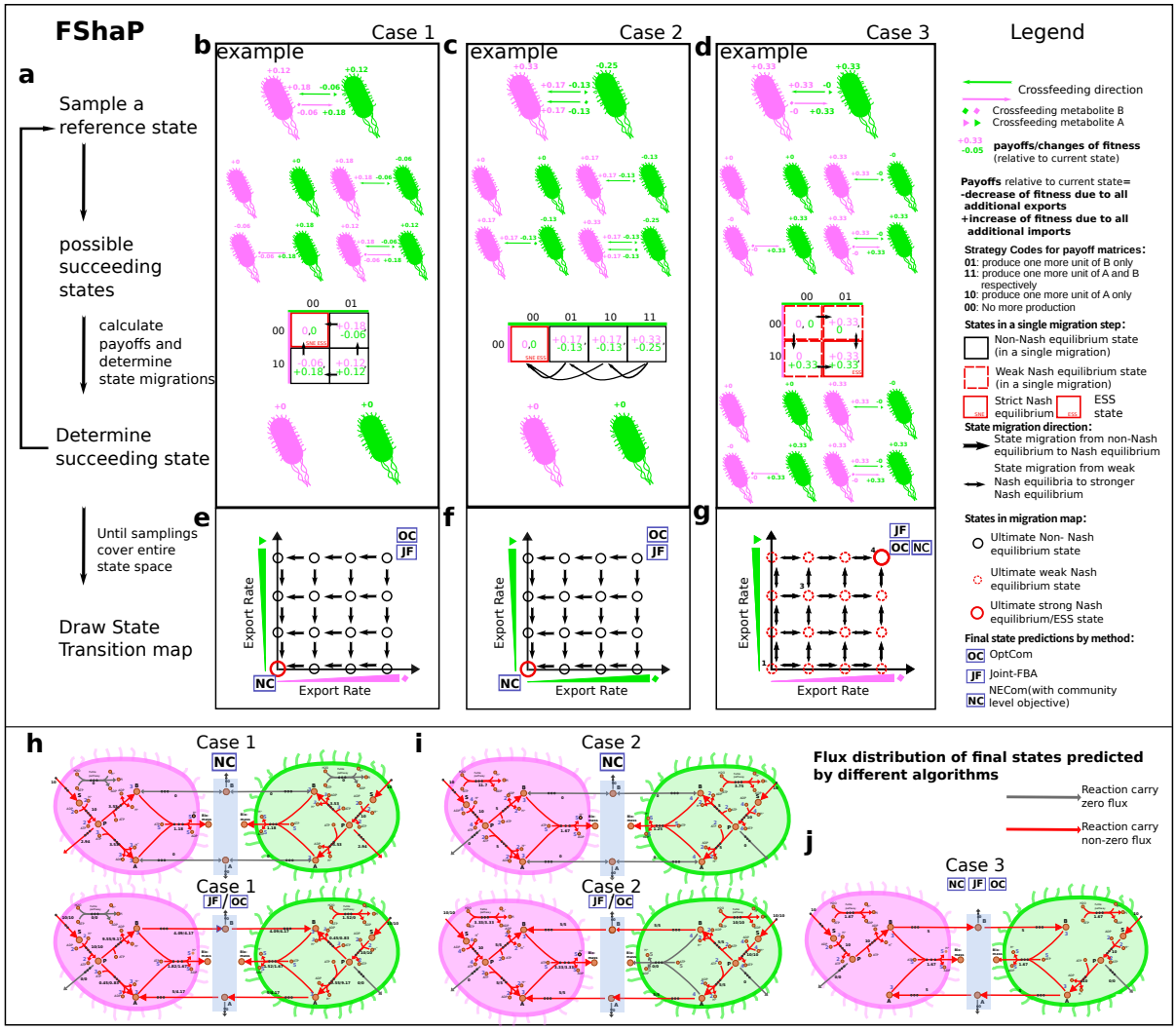

Figure 2. Transition of cross-feeding states predicted using FShaP. (a) Workflow of FShaP. **(b - d)** Example of determining the next cross-feeding state in a single state transition step for the three toy models. **(e - g)** The corresponding transition maps of cross-feeding state. Final (optimal) states predicted by joint-FBA (JF), OptCom (OC) and NECom (NC) are labeled. **(h - j)** The corresponding flux distributions predicted by the three algorithms. Specifically, **(h)** includes a toy community model consisting of two members, both capable of producing biomass precursors A and B, but at different ATP costs. **(i)** includes a toy community model consisting of two members, both capable of producing biomass precursors A and B, but has different biomass yields on these two precursors. **(j)** includes a toy community model consisting of two members, one capable of producing biomass precursors A but auxotrophic for B, the other capable of producing biomass precursors B but auxotrophic for A.

determined (examples as fig. 2b-d). It is worth noting that since strategies for interacting organisms can be inter-dependent, a strategy of export adopted by a community member can automatically trigger strategies of uptake for its partner(s),if doing so can increase the importer's fitness.

Transition map for metabolic cross-feeding states

State transition starting from a reference state, in order to gain a global view of state transition trend, different reference states were sampled (usually in a fixed step-size) within the state space shaped by environmental and physiological constraints. when the samples cover entire state space, a map can be generated in a vector field style to offer a global view of the trend and indicate (weak and strict) Nash Equilibria and ESS. The results can be compared with the predictions by Joint-FBA, OptCom, as well as NECom newly formulated in this study (described in the next subsection), which were all developed to predict the final optimized state.

Predicting global Nash Equilibrium of metabolic interactions using bi-level optimization approach

To find optimized cross-feeding states directly, as an alternative to FShaP, a bi-level optimization framework termed the Nash Equilibrium predictor for microbial Community (NECom) was developed. The biggest advance of NECom (fig. 3) in comparison with previous methods is the absence of 'forced altruism' constraint. While the inner problem is essential the FBA problem, the primary innovation lies in modeling how the availability of community metabolites to each microbe depends on the exchange profile (strategy) of each microbe. We proved mathematically that NECom prediction can guarantee Nash equilibria for its community members (**Supplementary Note**). With community biomass production as the outer-level objective function, solutions consistent with ESS or strict Nash equilibria can be found (in some cases ESS depends on the actual competition of substrates which in turn depends on uptake kinetics that is not modeled in this study). The community-level objective function was used in all NECom predictions in this study.

Evaluating FShaP and NECom with classical games

To validate the proposed algorithms in a simple and clear way, four toy models including classical cases in game theory are analyzed (first three shown in fig. 2). Case 1 is a community model consisting of two individual species (or mutants) with equal abundance named sp1 and sp2 (fig. 2h). Each species can yield ATP through converting substrate S (assumed to be sufficient) to intermediate P and subsequently consume ATP though converting P to biomass precursors A and B, which can be freely exchanged between the two species. The difference between them is that sp1 produces B more efficiently (consuming 1 ATP vs. 3 ATP for sp2), while sp2 produces A more efficiently (consuming 1 ATP versus 3 ATP for sp1), reflecting the existence of pathways with various yields commonly observed in nature. Intuitively the optimal strategy for the community is that each species cross-feeds each other with the metabolites produced at higher efficiency, i.e., sp1 supplies B to sp2, while sp2 feeds A to sp1, coinciding with the prediction by joint-FBA and OptCom

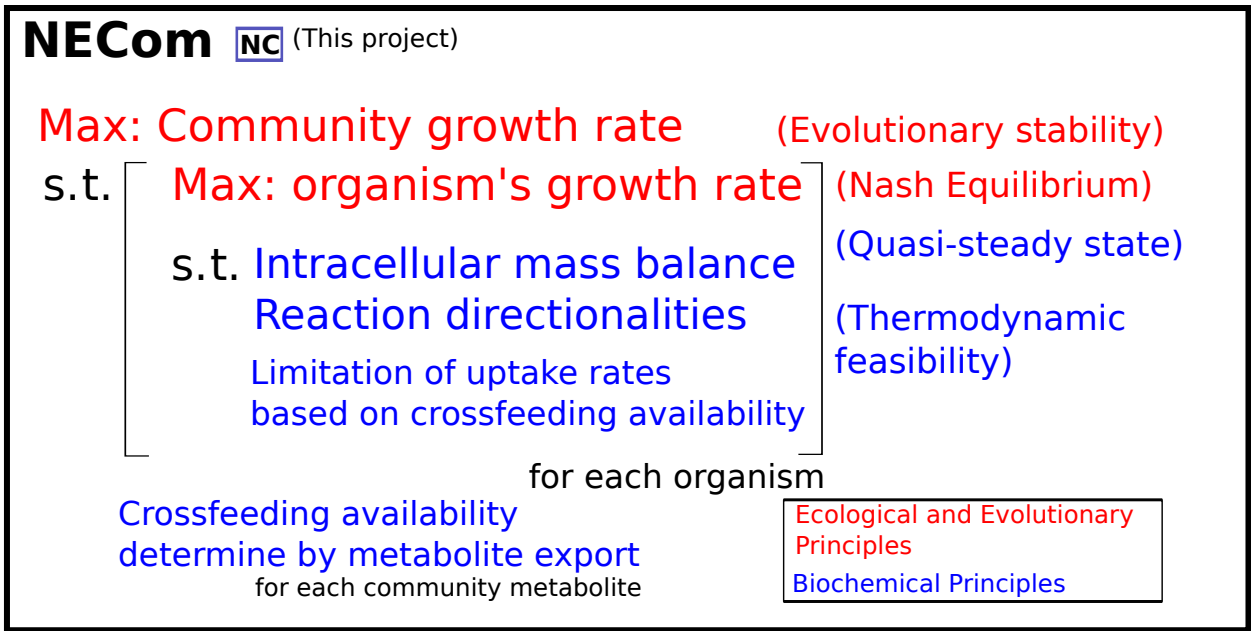

Figure 3. Schematic diagram of the NECom formulation

(the lower flux map in fig. 2h). However, it is not a NE since either species, say sp1, can have a mutant that does not excrete B but keeps consuming A and increases its own biomass production. In contrast, NECom predicts that the two species will grow at a lower rate and exchange nothing (the upper flux map in fig. 2h). Since there is no way for each species to grow faster given no export by another species, this is a NE. In analogy to classical matrix game, the payoff matrix corresponding to different cross-feeding states (fig. 2e) was constructed with the FShaP method. The payoff matrix indicates that maximum growth without cross-feeding ([00, 00]) is the (strict) NE as well as evolutionary stable strategy (ESS), which is a NE not invadable by other mutants (strategies). Any other strategy combinations including the complementary cross-feedings ([01,10]) predicted by Joint-FBA/OptCom are not stable and will eventually evolve to the NE.

The interaction in the toy community model analyzed above is characterized as a game called 'prisoner dilemma', because the NE is all members choosing 'defect' instead of 'cooperate', which NECom correctly predicts. The 'forced altruism' setup is the cause for the mutualistic prediction by joint-FBA and OptCom, because the setup artificially prioritizes the metabolite export by each member for its partner over the optimization of its fitness in order to achieve higher community-level fitness. FShaP returns the same unique NE as NECom for this toy model (fig. 2e).

Case 2 is a slight variant of case 1: the two organisms have different biomass yield on same precursors, also reflecting a norm in nature (different species have same biomass precursors such as essential amino acids or pyruvate, but biomass yield on them are different). Strategy transition map (fig. 2f) indicates that non-cross-feeding is strict Nash equilibrium/ESS, the same as the prediction by NECom. However, Joint-FBA

and OptCom predict the final state to be that species 2 exports all of its biomass precursors A and B to support the growth of species 1 (fig. 2i lower). Such results are the consequence of formulations that invoke 'forced altruism', which determine that doing so achieves the highest overall growth, despite that species 2 needs to completely sacrifice its own fitness.

Auxotrophy is common in microbial communities. Unlike the previous cases, auxotrophs relying on complementary cross-feeding for growth while the cross-feeding metabolites such as amino acids can be costly to produce. In such case how does cooperation become favorable or would defect still be the outcome despite no growth? Can cheaters and donors co-exist? In case 3, we used the same setup as in case 1 but removed the reaction for synthesizing metabolite A in sp1 and the reaction for synthesizing B in sp2 (fig. 2g). This mutualist-cheater case is a classical question of interest in ecology [62–65]. The payoff matrix in fig. 2d shows that four strategy combinations (i.e the mutualism, two commensalisms, and non-cross-feeding) are NE, but mutualism is the ESS and there is no strict NE. Therefore from the view of evolutionary game theory, the non-producing cheaters in this case can still co-exist with producer although not being able to outgrow them. This is another example to explain why mutualism or commensalism are possible even if it costs members some resource: because when a particular metabolite is not growth limiting, exporting the metabolite does not penalize the organism's fitness. In this case we checked that all NE identified by the payoff matrix are feasible solutions of NECom. The ESS is identical to the prediction of NECom (and OptCom/Joint-FBA).

Then we tested the algorithms applied to a community with more than two members in case 4 (fig. 4a). The community was constructed by adding sp3, an exact copy of sp2, to the toy model in case 3. sp2 and sp3 are dependent on the export of B by sp1 and sp1 is dependent on the export of A by the other two members. An interesting question is whether the symmetric pair sp2 and sp3 will both produce A at same time. Nash equilibrium predicted by NECom indicates that sp2 and sp3 will always choose opposite strategies, i.e., when sp2 produces A, sp3 does not and vice versa (note the symmetry between sp2 and sp3 in fig. 4b). This defining feature categorizes the interactions as a typical 'snowdrift game' between sp2 and sp3. This also explicitly demonstrates the conclusion of our analysis of case 3 that mutualists and cheaters can co-exist in a NE. This case also demonstrates that NECom has the potential to predict species/strains level heterogeneity caused by evolution

A real-world case study: co-culture system of *C. reinhardtii* and *S. cerevisiae*

Through toy model analysis we show that NECom is able to predict results that are consistent with traditional game-theoretical analysis. Next NECom is applied to a realistic algae-yeast co-culture system. Hom and Murray reported that two genetically distant species *C. reinhardtii* and *S. cerevisiae* can establish obligatory

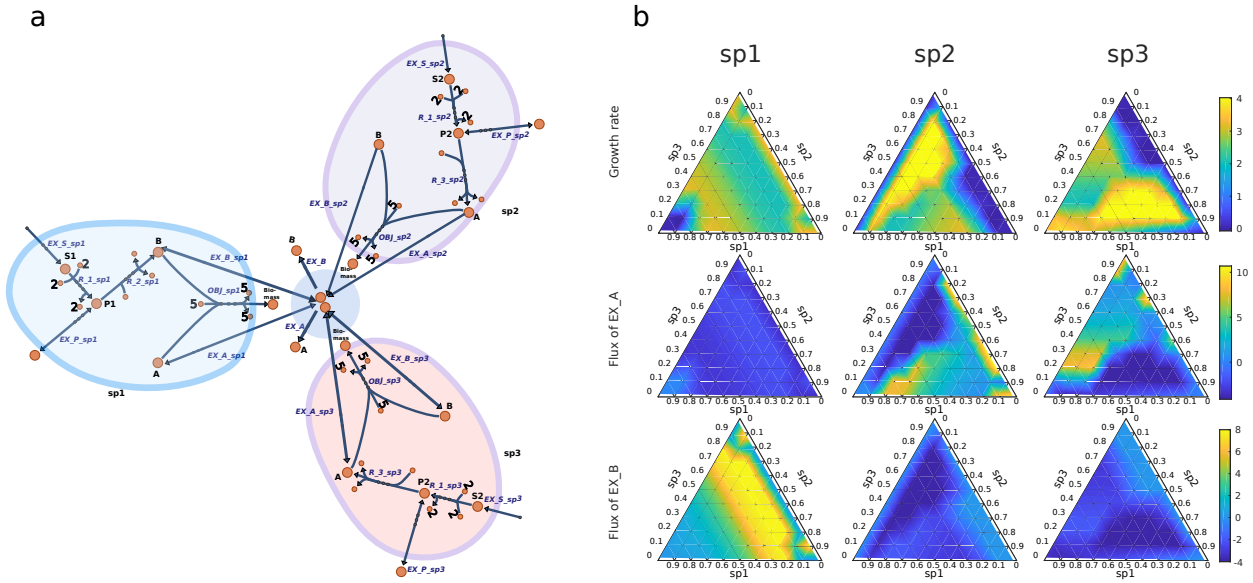

Figure 4. Toy community model and flux profiles in case 4. **(a)** Toy community consisting of three species. sp3 is a copy of sp2. They both depend on B produced by sp1, and sp1 depends on A produced by either or both of sp2 and sp3. **(b)** Growth rates and the cross-feeding reaction rates for each species under different relative abundance distributions.

symbiosis in simple media [66]. Their data show that *C. reinhardtii* almost always have a higher abundance than *S. cerevisiae* in all 80 experiments with different initial substrate concentrations. Within a wide range of initial concentrations of two key substrates (nitrite and glucose), these two species can co-exist for an extended time (≥10 days) period (**Supplementary fig.1**). The underlying growth-controlling interaction and many metabolic details remain to be elucidated in-depth, therefore NECom was applied to a community model integrating Yeast 7.6 [67] and *i*Cre1355 [68], genome-scale metabolic models for *S. cerevisiae* and *C. reinhardtii* respectively, to gain insights into the symbiotic interaction at the metabolic level after validation with the experimental results.

Verification of NECom

In order to verify the NECom method, prediction of the phenotype of *C. reinhardtii*-*S. cerevisiae* system by NECom and Joint-FBA were compared (fig. 5b) with measurement derived data (**Supplementary Note**) for the cases under a wide range of conditions (fig. 5a). The average Root squared mean error (RSME) for NECom is 0.0031 (h^{-1}) for predicting the growth of *C. reinhardtii* and 0.0085 for the growth of *S. cerevisiae*, significantly lower than the RSME of Joint-FBA (0.0088 and 0.048 respectively). The growth rates of *S. cerevisiae* predicted by Joint-FBA are generally significantly higher than the experimental results, leading to *S. cerevisiae* predicted as a generally faster grower while the experimental results indicate the opposite in majority of the cases. When the glucose uptake of *S. cerevisiae* is low (<0.6 mmol/gDWh), Joint-FBA

predicts positive values instead of the experimental negative values. These errors are caused by 'forced altruistic' constraints, which force *C. reinhardtii* model using photons to convert low energy carbon containing metabolites (primarily CO_2) released by *S. cerevisiae* to various energy richer substrates consumed by *S. cerevisiae* (example as fig. 5c). Based on FBA and under same condition, maximizing *S. cerevisiae*'s growth rate can yield 2.7 times greater community growth rate in average than maximizing *C. reinhardtii*'s growth rate. Therefore, 'forced altruistic constraints' unreasonably weaken the role of individual fitness and lead to inaccurate predictions. Although in most cases NECom agrees well with the measurement derived data, in some cases (e.g nitrite uptake = 0.225 mmol/gDWh, glucose uptake = 0.725 mmol/gDWh) *S. cerevisiae*'s growth is underestimated while *C. reinhardtii*'s growth is overestimated. It is probably due to over-estimated uptake rates of CO_2 by *C. reinhardtii*, resulting in more-than-actual ammonia converted to biomass and less-than-actual ammonia exported for *S. cerevisiae*'s growth. This kind of discrepancies is likely due to the absence of uptake kinetics in the current study. In the future uptake kinetics will be incorporated for better quantitative predictions.

Substrate uptake rates affect the relative growth rates of community members

Several features of the co-culture system can be concluded from the experimental results and NECom predictions provide additional interpretation for these observed features. As shown by the experimental results in fig. 6c, the correlation between growth rates of both community members and glucose uptake rates (by *S. cerevisiae*) suggests two interesting phenomena. First, *C. reinhardtii* almost always have positive growth while *S. cerevisiae* could have negative growth especially when its glucose uptake rate is low. The lower the glucose uptake is, the more advantage of *C. reinhardtii* can have over *S. cerevisiae*. The second phenomenon is the switch of growth advantage, in 76.7% of the experimental cases, *C. reinhardtii* has higher growth rate than yeast, but when glucose uptake is high (as indicated in fig. 6c, v_{glc}^{uptake} >0.8 mmol/gDWh), *S. cerevisiae* becomes the faster grower. This switch of growth advantage contributes largely to the stabilization of the community. Both of aforementioned phenomena are generally captured by NECom prediction (fig. 6d). Therefore we used the NECom simulated data to elucidate the potential cause of these phenomena.

Firstly we examined the always-positive growth of *C. reinhardtii*. Since only in low nitrite uptake rate region, the range of the experimental glucose uptake rate is wide enough for analysis, two low nitrite uptake rates were considered (0.025 and 0.075 mmol/gDWh, still representative since 67% of the experimental cases has estimated nitrite uptake rates lower than 0.1 mmol/gDWh). The ATP required for cellular maintenance (ATPM) for both species were computed. If the ATPM flux is lower than a minimal value (2.85 mmol/gDWh for *C. reinhardtii* and 7.5 mmol/gDWh for *S. cerevisiae*), the growth rate will be negative. We found that the

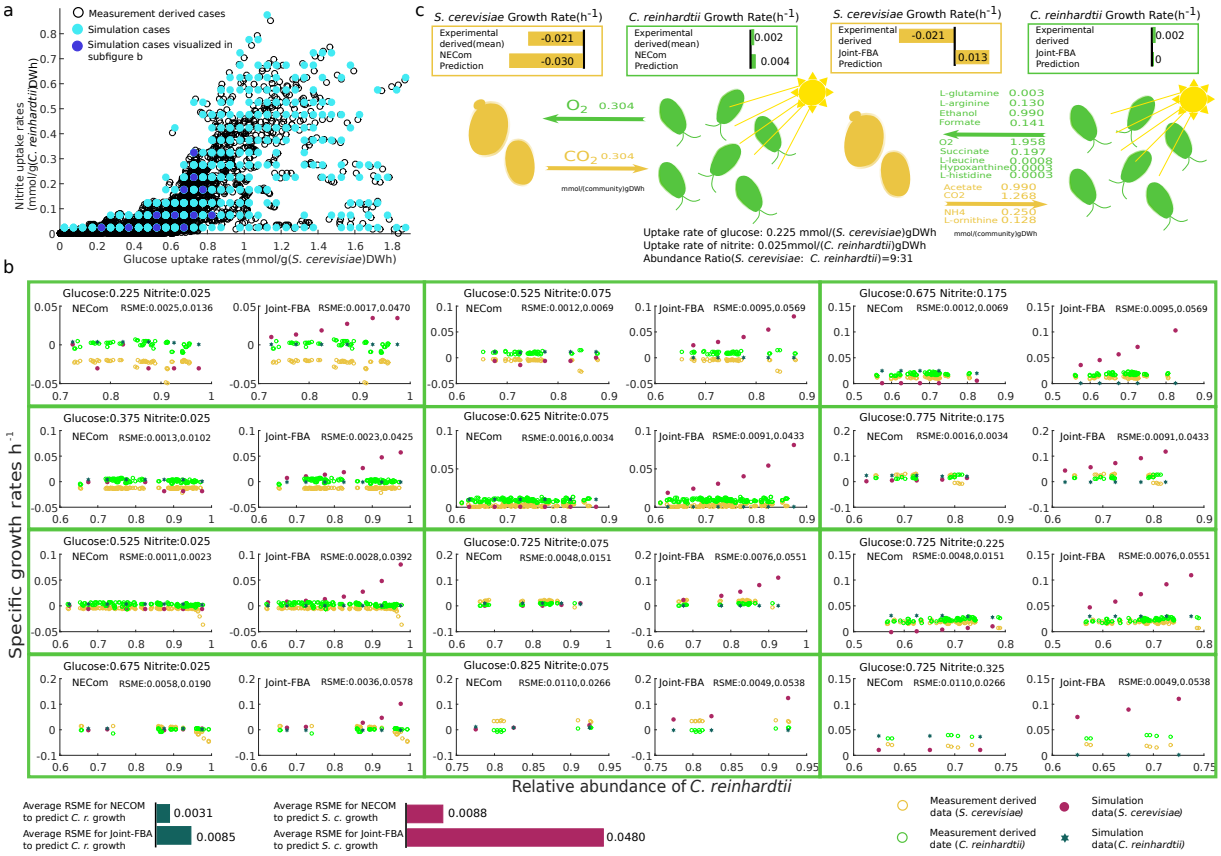

Figure 5. Verification of NECom and comparison with Joint-FBA. (a) Distribution of experimental and predicted cases in terms of the substrate uptake rates. Hallow circles represent the 3221 experimental cases (see Supplementary Note, noting that an axis of abundance is not presented in the figure, one circle can represent multiple cases with different abundances). Glucose and nitrite uptake rates were estimated based on the elemental composition of biomass and time series of cell counts (see Supplementary Note). (Dark and light) blue filled circles represent 488 simulation cases, which represent the experimental cases and with representativeness scores assigned (see Supplementary Note). **(b)** Simulation results of example cases (dark blue filled circles in (a)) using NECom and Joint-FBA compared with experimental cases. Rooted squared mean error (RSME) are calculated in each case. Weighted average RSMEs for both simulation methods are shown at the bottom. **(c)** Example demonstrating the difference of prediction between NECom and Joint-FBA in terms of predicted cross-feeding metabolites and its associated fluxes. RSMEs are labeled.

minimal ATPM flux is always satisfied for *C. reinhardtii*. However, for *S. cerevisiae*, when the glucose uptake rate drops below 0.8 mmol/gDWh (fig. 6b), the ATPM flux starts to drop below the minimal requirement, the gap keeps increasing as the glucose uptake rate continues to decrease. We believe that the reason for this difference lies in the different source of energy used for fueling ATPM by the two species. For *C. reinhardtii* the energy source is photons while for *S. cerevisiae* the energy originates from metabolizing glucose. In the experiment, illumination dose not change but the glucose concentration has different initial values and decreases with time, supporting our analysis.

Secondly, the reason for why *S. cerevisiae* narrowed its growth rate gap between *C. reinhardtii* and even surpassed the latter is that, the carbon flux to the biomass of *S. cerevisiae* and nitrogen flow to the biomass of *C. reinhardtii* have opposite trends to the increase of glucose uptake rate. Based on NECom prediction, responding to the increasing glucose uptake rates*S. cerevisiae* has an increasing ratio of ATP for biomass synthesis to ATP for cellular maintenance, leading to an increasing growth rate fig. 6f). In the mean time, there is a higher carbon flow to biomass at the cost of lower flow to exported CO_2, resulting in relatively less carbon available for *C. reinhardtii* to synthesize its biomass (fig. 6e). In the aspect of *C. reinhardtii*, nitrogen flux has the exact opposite trend. The nitrogen flowing to exported ammonia has increasing share while the nitrogen flux for *C. reinhardtii*'s growth keeps decreasing (fig. 6g). This trend becomes more apparent when *C. reinhardtii*'s nitrite uptake rate is low. Increasing the share of nitrogen flux to exported ammonia instead of its own growth seems to contradict our intuition that the organism's flux distribution should prioritize its own fitness. However, in this particular interacting case, such adjustment of nitrogen distribution does have advantage on *C. reinhardtii* itself, since CO_2 and photons instead of nitrite are the limiting substrates for *C. reinhardtii* (fig. 7d). Increasing nitrogen exported for *S. cerevisiae* can increase its export of CO2, which in turn benefits *C. reinhardtii*'s growth.

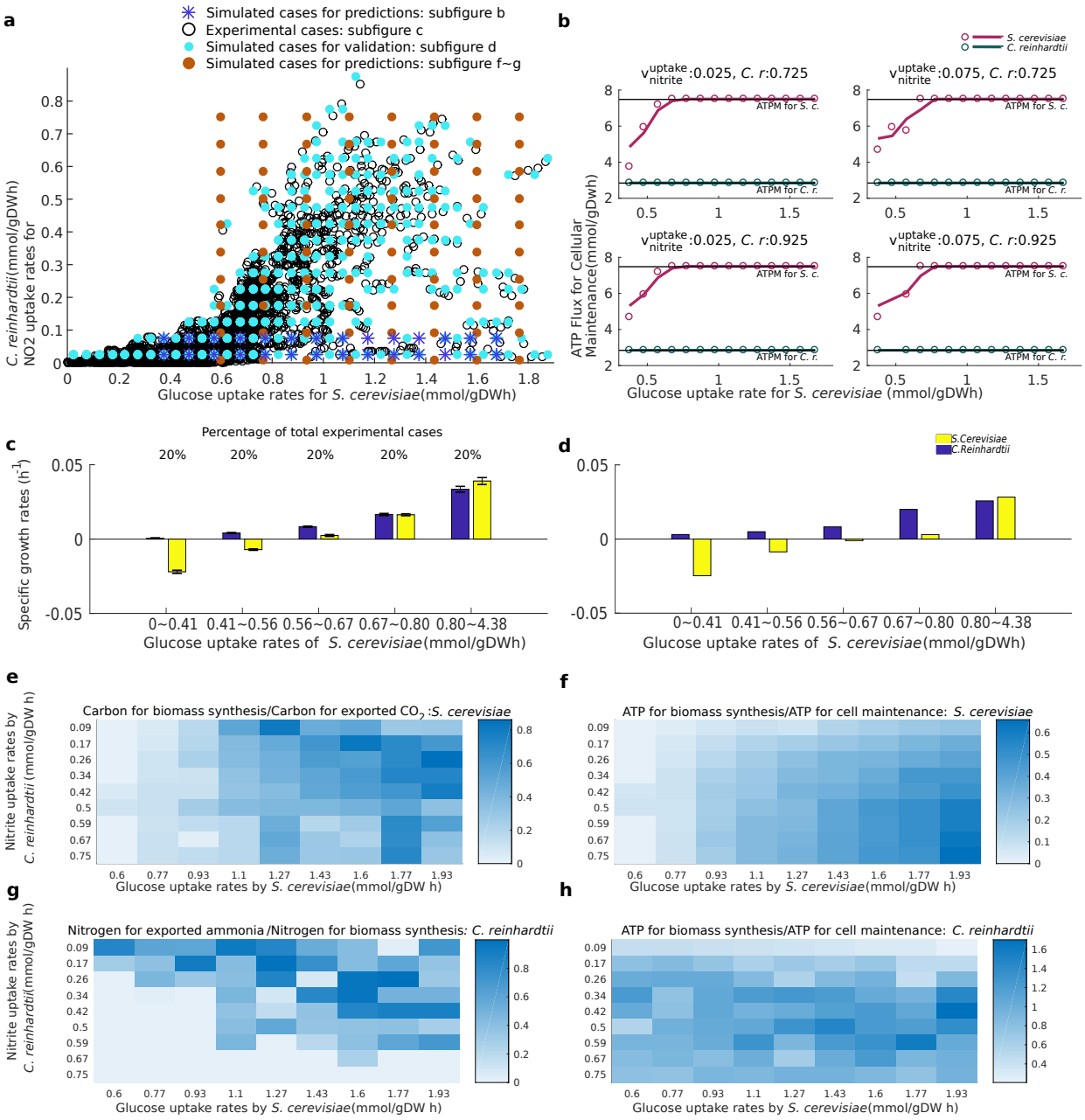

Figure 6. Mass and energy flow analysis. (a) Experimental and simulation data distribution. Hollow circles and light blue filled circles are set up in the same way as fig. 5a. Brown filled circles represent NECom predictions at various *C. reinhardtii*'s relative abundances, 631 cases in total**Supplementary Note**. Dark blue asterisks represent simulation cases for ATP analysis shown in (b). For each point, simulations were performed at two different *C. reinhardtii* abundances (0.725 and 0.925). **(b)** ATP consumed for the cellular maintenance of *C. reinhardtii* and *S. cerevisiae* as a function of the glucose uptake rate for *S. cerevisiae* with the nitrite uptake rate and abundance of *C. reinhardtii* fixed at different values. **(c)** Average specific growth rate of *C. reinhardtii* and *S. cerevisiae* from experimental data (represented by the hallow circles shown in fig. 5a, which are grouped into five intervals of glucose uptake rate, each interval includes 20% of the experimental data. **(d)** Weighted average specific growth rate of *C. reinhardtii* and *S. cerevisiae* over simulations represented by light blue filled circles (488 cases in total). The weight is the representativeness score explained in **Supplementary Note**. **(e - h)** NECom-predicted distribution of elemental flows and energy flows, using simulation cases (represented by brown filled circles in **a**) covering a wide range of glucose and nitrite uptake rates where experimental cases are sparsely distributed.

Predicted negative frequency-dependent dynamics caused by limiting cross-feeding metabolites

Negative frequency-dependent dynamics (or selection at evolutionary scales) is a type of community stabilizing mechanism that allows the species with lower abundance to thrive. When *S. cerevisiae*'s glucose uptake rate is low (<0.6 mmol/gDWh), *C. reinhardtii*'s growth rate is significantly higher than yeast, but not sensitive to the variation in abundance (fig. 5b). However, NECom predicts that with higher glucose uptake rates (>0.75 mmol/gDWh) the growth rates of the two species will have opposite trends as the relative abundance of *C. reinhardtii* and often there exists a point of equal growth rate (black circles in fig. 7a), where the faster and slower growing species are swapped. Such a growth-abundance relationship is negative frequency-dependent, which stabilizes the co-existence of interacting species by dynamically evolving to the equal-growth-rate population steady state. An interesting observation is that the population steady state shifts toward the left on the abundance axis with the increase of glucose uptake rate for *C. reinhardtii* (fig. 7a), indicating that the growth of *S. cerevisiae* gains advantage over *C. reinhardtii* with an increasing glucose uptake rate. The prediction is consistent with the experimental data (fig. 6c).

We speculate that the changing availability of some key substrates might be the reason for the negative frequency dependent dynamics and the shift of population steady state. To test our speculation, all cross-feeding metabolites and externally sourced substrates need to be considered. We ask what metabolites are the major substrates used by the two species. Among the simulation cases at various glucose uptake rates, nitrite uptake rates and abundances(represented by brown dots in fig. 6a), cross-feeding metabolites observed include O_2, CO_2, ammonia, acetate and succinate. The former three metabolites occur in 93% of the total cases (fig. 7b). Therefore, O_2, CO_2, ammonia together with external sourced substrates including photon, glucose and nitrite are selected for further analysis. Since only limiting substrates can have impact on community members' growth, in order to specify which substrates are growth-limiting, shadow prices for the uptake of each metabolites are calculated. A positive shadow price indicates the corresponding metabolite has impact on cellular growth at a given state and the value indicates the intensity of such impact. We found that for *C. reinhardtii*, CO_2 is a limiting metabolite under almost all simulated conditions (fig. 7d). Photons have significant limiting effect when both nitrite and glucose uptakes are low, but almost shows no limiting effect when nitrite uptake is high (>0.6 mmol/gDWh). Nitrite is generally not limiting. For *S. cerevisiae*, only ammonia exhibits significant limiting effect (fig. 7e). Since photon's availability is constant, we focus on analyzing how CO_2 and ammonia affect the growth rates of this system.

fig. 7f-i indicate that with increase in the abundance of *C. reinhardtii*, CO_2 supplied by *S. cerevisiae* decreases, causing decrease in the growth rate of *C. reinhardtii* since CO_2 is the limiting substrate confirmed by the

positive shadow price curve. In the meantime, increase in ammonia supply from *C. reinhardtii* contributes to the increasing growth rates of *S. cerevisiae*, since ammonia uptake has increasingly positive shadow prices. Therefore, the opposite trends in the supply rate of each limiting substrates are responsible for the observed negative frequency-dependent dynamics.

Shadow price analysis can also explain why the population steady state changes with the glucose uptake rate. fig. 7a shows that with the increase in glucose uptake rate, the two growth-abundance curves becomes steeper at low *C. reinhardtii*'s abundance (<0.6mmol/gDWh), causing the cross point shifting to the left. The steepness of a growth-abundance curve is proportional to the shadow price for limiting substrate uptake. Comparison of fig. 7g and fig. 7f reveals that, fixing the nitrite uptake rate at 0.09 mmol/gDWh and increasing the glucose uptake rate from 0.93 mmol/gDWh to 1.93 mmol/gDWh result in an increase in shadow price for CO_2 uptake by *C. reinhardtii* from 0 to 0.02 0.04 gDW/mmol when the abundance of *C. reinhardtii* is below 0.6. Similarly fig. 7i and fig. 7h indicate that if the nitrite uptake rate is fixed at 0.59 mmol/gDWh, shadow prices for ammonia uptake by *S. cerevisiae* will increase from 0 to 0.25 gDW/mmol when the abundance of *C. reinhardtii* is below 0.7.

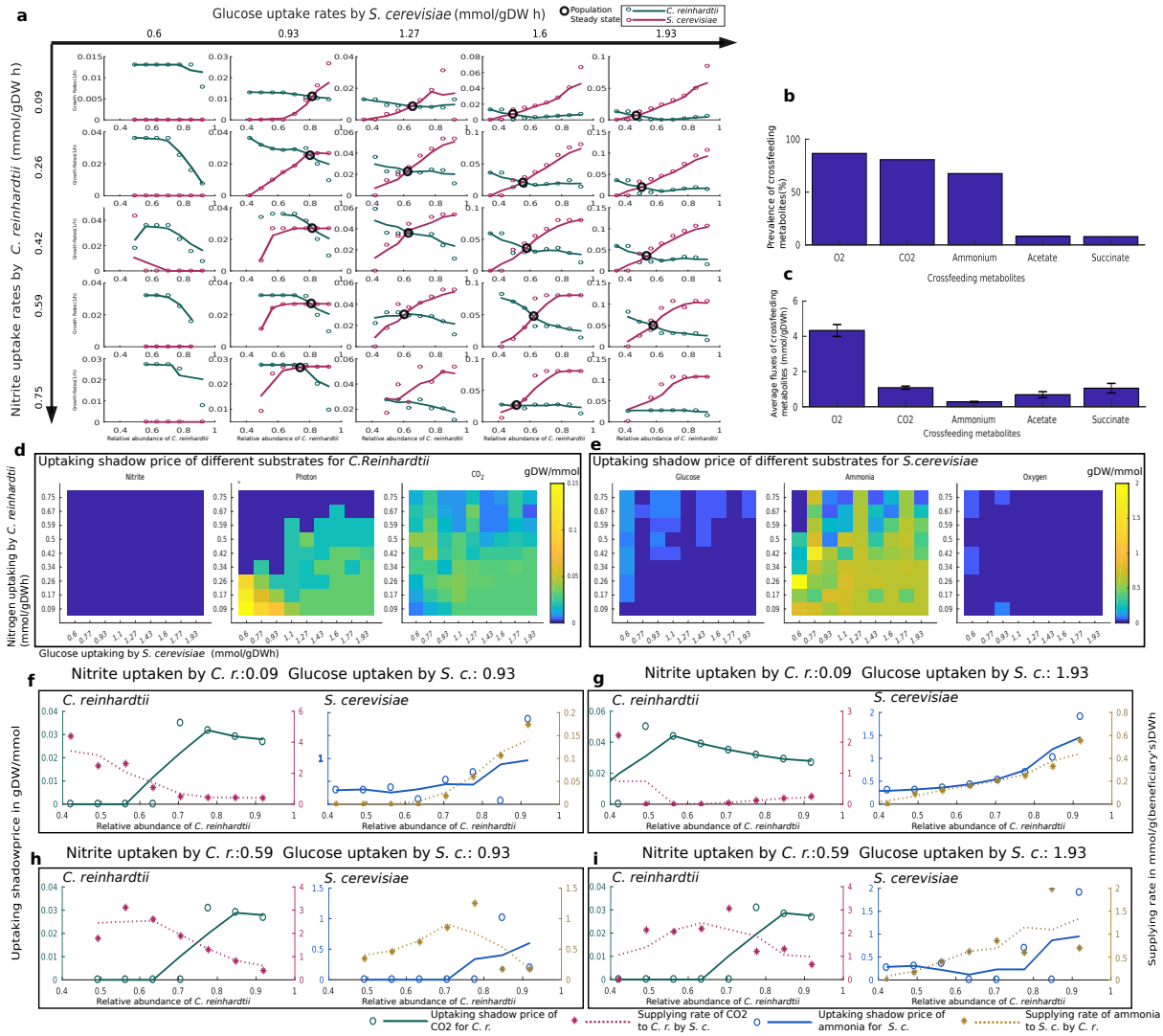

Figure 7. Shadow price based limiting substrate analysis. Simulation cases referred in this figure are those represented by brown filled circles in fig. 6a. **(a)** Growth rates of *C. reinhardtii* and *S. cerevisiae* as functions of the relative abundance of *C. reinhardtii*, at medium to high glucose uptake rates. **(b - c)** Prevalence and average flux of each cross-feeding metabolites across all simulation cases. **(d - e)** Average shadow price of major substrate uptake (including cross-feeding metabolites) by *C. reinhardtii* and *S. cerevisiae* under various nitrite and glucose uptake rates. **(f - g)** Shadow prices and supply rates of cross-feeding CO_2 for *C. reinhardtii*, and ammonia for *S. cerevisiae* as functions of the relative abundance of *C. reinhardtii*.

Relations to previous methods

A game-theoretical method has been proposed recently to determine Nash equilibria for interacting organisms using metabolic models [49]. In that proposed method, the Black Queen hypothesis [69] was tested by checking whether the existence of auxotrophic mutants is favored by evolution if there is leakage of metabolites. Metabolite leakage was predefined and uptake of leaky metabolites was determined using a distribution rule. FBA was then performed for each genotype in the population to compute the payoff matrix which was subsequently used for Nash equilibrium determination as well as dynamic simulation using the replicator equation. While the results elegantly captured *S. cerevisiae*'s invertase system and suggested potential auxotrophic pairs that can stably co-exist, performing FBA for each individual genotype, or more generally organism, does not allow individuals to 'sense and response' to each other via changes in the metabolic environment. Therefore, the possible interactions observed are confined to the cross-feeding of the predefined leaky metabolites. In the current study, the Black Queen hypothesis is not invoked (though it can be). Also, by clearly defining the concept of microbial metabolic games and the unique strategy space which is a continuous flux space constrained by the strategies of other players, we developed two algorithms to search the interdependent continuous flux space to determine Nash equilibria among all available interactions. NECom achieves this by using a bi-level framework, in which each organism optimizes its own fitness, under the substrate uptake constraints shaped by the strategies of other community members. FShaP provides an alternative approach based on iterative shadow price analysis, such that the strategies of individuals and the metabolic environment change interactively until a Nash equilibrium is reached. In relation to previous algorithms for simulating community metabolic models, OptCom [43] also employs a bi-level optimization framework but the main innovation of NECom lies in the introduction of outer variables to constrain the uptake only for the inner problems instead of both uptake and export (see Methods for the mathematical details). SteadyCom [70] implements a population steady state but the single objective function also unavoidably imposes forced altruism on the community the same way as joint-FBA does. We have not implemented the population steady state in the formulation but it can still be analyzed by fixing the relative abundances at different values as performed in the algae-yeast case study.

Conclusion

We developed a bi-level optimization algorithm called 'NECom' to predict the Nash equilibrium of multiple species' interacting game at the metabolic level. In order to compare NECom prediction with those obtained from traditional game theory analysis, a method termed 'FShaP' is proposed to construct the payoff table of inter-species metabolic interaction to analyze cross-feeding state transition. NECom was shown to predict

Nash equilibria of different types of classical games correctly in toy models that previous methods' predictions cannot guarantee. The main reason for this difference is that NECom does not contains any 'forced altruism' setup that computationally forces individual species to fulfill other species's metabolic need before their own. NECom, using modern mixed integer programming technology, has the potential to efficiently search for Nash equilibria in large scale and complex systems, but it does not predict the strategy transition path as revealed by the FShaP approach. The two methods are complementary and useful for bridging traditional evolutionary game theory and metabolic models for in-depth analysis of inter-cellular interactions. For the co-culturing system of *C. reinhardtii* and *S. cerevisiae*, with minimal information from the experimental data, NECom is able to reveal that the decreasing glucose concentration vs. the constant photon availability provides significant growth advantage of *C. reinhardtii* over *S. cerevisiae*; CO_2 and ammonia are growth-limiting cross-feeding substrates for *C. reinhardtii* and *S. cerevisiae* respectively; and the negative frequency-dependent growth pattern is cause by opposite trends of the supply rates of each species's limiting substrates.

Methods

FBA Shadow price based Payoff matrix (FShaP)

After chosen a starting cross-feeding state, the relative payoff of a specific strategy combo can be calculated by summing the impacts of all export and uptake on the chosen community member ('species 1'):

$$E(S1_p, S2_q) = -\overbrace{\sum_{i \in I^{ex}} (\mu^{LB}_{com(i,1),1} s1_{i,p})}^{\text{cost of 1 additional export}} + \overbrace{\frac{X_2}{X_1} \sum_{i \in I^{ex}} (\mu^{LB}_{com(i,1),1} s2_{i,q})}^{\text{benefit of corresponding additional import}} \qquad i \in I^{ex}, p, q \in P \tag{1}$$

$$E(S2_q, S1_p) = -\sum_{i \in I^{ex}} (\mu^{LB}_{com(i,2),2} s2_{i,q}) + \frac{X_1}{X_2} \sum_{i \in I^{ex}} (\mu^{LB}_{com(i,2),2} s1_{i,p}) \qquad i \in I^{ex}, p, q \in P \tag{2}$$

where $E(S1_p, S2_q)$ is the payoff for species 1 while interacting with species 2, they carry strategy combo p and q respectively. $E(S2_q, S1_p)$ is the payoff for species 2 while interacting with species 1, and they carry strategy combo q and p respectively. Each strategy combo contains strategy 0-1 binary indicator $s1_{i,p}$ or $s2_{i,p}$, for which '1' represents exporting one more unit of metabolite i, and 0 for not exporting, X_1 and X_2 denoting the relative abundance of species 1 and species 2 respectively, subject to $X_1 + X_2 = 1$, $X_1, X_2 \in [0, 1]$. I^{ex} is the set of cross-feeding metabolites, and $com(i, 1)$ and $com(i, 2)$ are the indices of exchange reaction for metabolite i for species 1 and 2 respectively. $\mu^{LB}_{com(i,n),n}$, the shadow price of the exchange reaction $com(i, n) \in J^{ex}$, can be retrieved from the solution of dual problem of FBA, which can be derived from the primer problem of FBA. Let N be the set of organisms in a microbial community, for each organism $n \in N$, let I_n be the set of metabolites and J_n be the set of reactions, $\boldsymbol{c_n}$ be the objective indicator vector, in which 1 indicates the corresponding flux variable $v_{j,n} \in V_n$ of reaction j is the objective and 0 for otherwise.The primer problem of FBA can be formulated as:

$$\max \boldsymbol{c_n} V_n$$

subject to

$$\sum_{j \in J_n} S_{i,j,n} v_{j,n} = 0 \qquad \forall i \in I_n, \forall n \in N \tag{3}$$

$$-v_{j,n} \leq -LB_{j,n}, \qquad \forall j \in J_n, \forall n \in N \tag{4}$$

$$v_{j,n} \leq UB_{j,n}, \qquad \forall j \in J_n, \forall n \in N \tag{5}$$

$$v \in \mathbb{R}$$

Where $v_{j,n}$ is the flux of reaction j, $S_{i,j,n}$ is the stoichiometry of metabolite i for reaction j , $LB_{j,n}$ and $UB_{j,n}$ are the lower bound and upper bound for the flux of reaction j, respectively. All subscripts n stand for organism n. The dual problem can be derived as:

$$
\begin{aligned}
&\min \sum_{j \in J_n} (UB_{j,n}\mu_{j,n}^{UB} - LB_{j,n}\mu_{j,n}^{LB}) \\
&\text{subject to} \\
&\sum_{i \in I_n} S_{i,j,n}\lambda_{i,n} + \mu_{j,n}^{UB} - \mu_{j,n}^{LB} = c_{j,n}, \qquad \forall j \in J_n, \forall n \in N \qquad (6) \\
&\mu^{LB}, \mu^{UB} \geq 0, \lambda \in \mathbb{R}
\end{aligned}
$$

Where μ_{LB} and μ_{UB} are the shadow price for the lower bounds constraints eq. (4) and the upper bounds constraints eq. (5) respectively, λ_n are the dual variable for eq. (3). in order to match the dual problem to a specific cross-feeding state, the lower bounds and upper bounds of cross-feeding reactions must be equal to the value of corresponding cross-feeding fluxes. With the payoffs computed by eq. (1) and eq. (2), the payoff matrix can be constructed as:

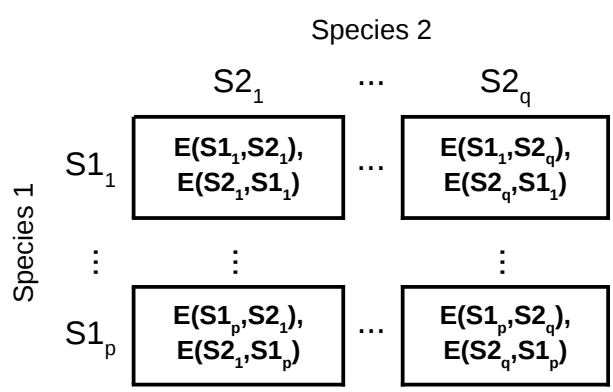

Figure 8. The general layout of payoff matrix of two interacting organisms. In each cell there are two payoffs. The first one is the payoff to species 1 upon its encounter with species 2. The second one is the payoff to species 2 upon its encounter with species 1.

NECom

Here we derive the bi-level optimization framework NECom, starting with the description of flux balance analysis (FBA) as the inner problem for optimizing the fitness of individual organisms. A set of outer-level variables to indicate the availability of metabolites for uptake are then introduced to connect the inner-level flux variable.Let I_n^{ex} be the set of extracellular metabolites in the community, $J_n^{ex} \subseteq J_n$ be the set of exchange

reactions between the community and organism n. Define an index mapping functions $I_n^{ex} \rightarrow J_n^{ex}$ such that $com(i,n) \in J_n^{ex}$ map extracellular metabolite $i \in I_n^{ex}$ to its corresponding exchange reaction. For each individual organism, we split the exchange reaction flux for a possible cross-feeding metabolite $v_{com(i,n),n}$ into two non-negative continuous variable: the uptake rate $v_{com(i,n),n}^{ut}$ and the export rate $v_{com(i,n),n}^{ex}$:

$$v_{com(i,n),n} + v_{com(i,n),n}^{ut} - v_{com(i,n),n}^{ex} = 0 \qquad \forall i \in I_n^{ex}, \forall n \in N$$

To explicitly model the mutual dependency in terms of inter-organism metabolite exchange, uptake of a metabolite by an organism is possible only if there is surplus of the metabolite in the medium after the consumption/production by the rest of the community:

$$X_n v_{com(i,n),n}^{ut} \leq \max\{v_i^{med} + \sum_{k \in N, k \neq n} X_k v_{com(i,n),n}, 0\} \forall i \in I_n^{ex}, \forall n \in N \tag{7}$$

Where X_n is the relative abundance of organism n (a pre-set parameter), which is multiplied by specific uptake rate $v_{com(i,n),n}^{ut}$ to correctly normalize the exchange with the community, and v_i^{med} is the maximum community uptake of metabolite i from the medium. Here to avoid forced altruism, $v_{com(i,n),n}^{ex}$ is designated as an inner variable independent of the outer problem, while the uptake rate $v_{com(i,n),n}^{ut}$ is also an inner variable but depends on the net availability of metabolite i. In this way we can ensure that individual organisms have 'autonomy' over their metabolite exports. Maximization of the community fitness in the outer level cannot force an organism to produce a certain metabolite unless FBA determines that the metabolite is necessary for, or at least not undermining the maximum growth of the organism. The max function in the eq. (7) is linearized by introducing an outer continuous variable $\beta_{i,n}$ and an outer binary variable $\delta_{i,n}$:

$$\left[\begin{array}{l} \beta_{i,n} \geq v_i^{med} + \sum_{k \in N, k \neq n} X_k v_{com(i,n),n} \\ \beta_{i,n} \leq (1 - \delta_{i,n})M + v_i^{med} + \sum_{k \in N, k \neq n} X_k v_{com(i,n),n} \\ \beta_{i,n} \leq \delta_{i,n} M \\ \beta_{i,n} \geq 0 \end{array}\right] \forall i \in I_n^{ex}, \forall n \in N \tag{8}$$

Where M is a large constant. In combination of inner problem and outer problem the complete formulation

of NECom can be written as:

$$NECom \tag{9}$$

$$\left[\begin{array}{lll} \max \quad v_n^{biomass} & & \\ \text{subject to} & & \\ \quad \sum_{j \in J_n} S_{i,j,n} v_{j,n} = 0, & \forall i \in I^n & \\ \quad LB_{j,n} \leq v_{j,n} \leq UB_{j,n} & \forall j \in J_n & \forall n \in N \\ \quad v_{com(i,n),n} + v^{ut}_{com(i,n),n} - v^{ex}_{com(i,n),n} = 0 & \forall i \in I_n^{ex} & \\ \quad X_n v^{ut}_{com(i,n),n} \leq \beta_{i,n} & \forall i \in I_n^{ex} & \end{array}\right] \tag{10}$$

$$\beta_{i,n} \geq v_i^{med} + \sum_{k \in N, k \neq n} X_k v_{com(i,k),k} \qquad \forall i \in I_n^{ex} \tag{11}$$

$$\beta_{i,n} \leq \delta_{i,n} M + v_i^{med} + \sum_{k \in N, k \neq n} X_k v_{com(i,k),k} \qquad \forall i \in I_n^{ex} \tag{12}$$

$$\beta_{i,n} \leq (1 - \delta_{i,n}) M \qquad \forall i \in I_n^{ex} \tag{13}$$

$$v \in \mathbb{R}; v^{ut}, v^{ex}, ub \geq 0; \delta \in [0, 1]$$

In the incidence where the above algebraic system is not feasible, one or more member cannot satisfy the minimal requirement of Non growth associated maintenance (NGAM), which is represented as a direct ATP consumption reaction with a pre-defined lower bound in model,negative growth or 'cell death' should occur, in order to enable NECom to predict this phenomenon, we separate community member in two sets based on NECom solution: let N^G be the set of community member(s) which has adequate substrate(s) to uptake to satisfy its NGAM, N^D be the set of the rest community member(s) that is dying due to insufficient nutrients, for the later case, the objective should not be set to maximization of biomass since it is a non-negative variable in model but must be non-positive,instead, maximization of its NGAM is believe as an reasonable objective function since it can be regarded as the struggling to surviving in nutrient scarce environment by maximization of energy production. Therefore we upgraded NECom enabling negative growth prediction

(NEComwNG) as:

$$NEComwNG \tag{14}$$

$$\left[\begin{array}{ll} \max \quad v_n^{biomass} & \\ \text{subject to} & \\ \sum_{j \in J_n} S_{i,j,n} v_{j,n} = 0, & \forall i \in I^n \\ LB_{j,n} \leq v_{j,n} \leq UB_{j,n} & \forall j \in J_n \\ v_{com(i,n),n} + v^{ut}_{com(i,n),n} - v^{ex}_{com(i,n),n} = 0 & \forall i \in I_n^{ex} \\ X_n v^{ut}_{com(i,n),n} \leq \beta_{i,n} & \forall i \in I_n^{ex} \end{array}\right] \quad \forall n \in N^G \tag{15}$$

$$\left[\begin{array}{ll} \max \quad v_n^{ATPM} & \\ \text{subject to} & \\ \sum_{j \in J_n} S_{i,j,n} v_{j,n} = 0, & \forall i \in I^n \\ LB_{j,n} \leq v_{j,n} \leq UB_{j,n} & \forall j \in J_n \\ v_{com(i,n),n} + v^{ut}_{com(i,n),n} - v^{ex}_{com(i,n),n} = 0 & \forall i \in I_n^{ex} \\ X_n v^{ut}_{com(i,n),n} \leq \beta_{i,n} & \forall i \in I_n^{ex} \end{array}\right] \quad \forall n \in N^D \tag{16}$$

$$\beta_{i,n} \geq v_i^{med} + \sum_{k \in N, k \neq n} X_k v_{com(i,k),k} \quad \forall i \in I_n^{ex} \tag{17}$$

$$\beta_{i,n} \leq \delta_{i,n} M + v_i^{med} + \sum_{k \in N, k \neq n} X_k v_{com(i,k),k} \quad \forall i \in I_n^{ex} \tag{18}$$

$$\beta_{i,n} \leq (1 - \delta_{i,n}) M \quad \forall i \in I_n^{ex} \tag{19}$$

$$v \in \mathbb{R}; v^{ut}, v^{ex}, ub \geq 0; \delta \in [0, 1]$$

Software and hardware used in the study

simulation for study of *C. reinhardtii*-*C. reinhardtii* interactions ran on a Linux server with 2 Intel Xeon E5-2680-V4 CPUs, with Baron Solver [71], all other computing ran on a Linux machine with an Intel i7-4800mq CPU. Pathway maps are originally generated in Escher Map [72]. All scripts were written in Matlab language.

Code and data availability

Data files and example codes will be available on https://github.com/Jingyi-Cai/NECom-FShaP.git

Acknowledgments

We acknowledge Dr. Wenyan Yuan, Dr. Erik F. Y. Hom, Dr. Guang Cheng, Dr. Xueying Ni and Ying Zhu for their useful comments. We acknowledge Dr. Nikolaos Sahinidis for his provision of an evaluation license for Baron solver and his quick fix in response to our bug reports.

Author contributions

J.C and S.H.J.C conceived and designed the study, J.C conducted all simulation studies and analyses. J.C and S.H.J.C prepared figures and wrote the manuscript. All authors critically reviewed and revised the manuscript.

Competing interests

The authors declare no competing interests

References

1. Lawrence, D. et al. Species interactions alter evolutionary responses to a novel environment. PLoS Biology **10**, e1001330 (2012).

2. Fiegna, F., Moreno-Letelier, A., Bell, T. & Barraclough, T. G. Evolution of species interactions determines microbial community productivity in new environments. The ISME Journal **9**, 1235–1245 (2014).

3. Pande, S. & Kost, C. Bacterial unculturability and the formation of intercellular metabolic networks. Trends in Microbiology **25**, 349–361 (2017).

4. McCutcheon, J. P. & Moran, N. A. Parallel genomic evolution and metabolic interdependence in an ancient symbiosis. Proceedings of the National Academy of Sciences **104**, 19392–19397 (2007).

5. Paterson, S. et al. Antagonistic coevolution accelerates molecular evolution. Nature **464**, 275–278 (2010).

6. Hillesland, K. L. & Stahl, D. A. Rapid evolution of stability and productivity at the origin of a microbial mutualism. Proceedings of the National Academy of Sciences **107**, 2124–2129 (2010).

7. Hillesland, K. L. et al. Erosion of functional independence early in the evolution of a microbial mutualism. Proceedings of the National Academy of Sciences **111**, 14822–14827 (2014).

8. D'Souza, G. & Kost, C. Experimental evolution of metabolic dependency in bacteria. PLOS Genetics **12**, e1006364 (2016).

9. Zhou, K., Qiao, K., Edgar, S. & Stephanopoulos, G. Distributing a metabolic pathway among a microbial consortium enhances production of natural products. Nature Biotechnology **33**, 377–383 (2015).

10. Chen, Z., Sun, X., Li, Y., Yan, Y. & Yuan, Q. Metabolic engineering of escherichia coli for microbial synthesis of monolignols. Metabolic Engineering **39**, 102–109 (2017).

11. Kamada, N., Chen, G. Y., Inohara, N. & Núñez, G. Control of pathogens and pathobionts by the gut microbiota. Nature Immunology **14**, 685–690 (2013).

12. Gilbert, J. A. et al. Microbiome-wide association studies link dynamic microbial consortia to disease. Nature **535**, 94–103 (2016).

13. Vandeputte, D. et al. Quantitative microbiome profiling links gut community variation to microbial load. Nature (2017).

14. Sommer, F., Anderson, J. M., Bharti, R., Raes, J. & Rosenstiel, P. The resilience of the intestinal microbiota influences health and disease. Nature Reviews Microbiology **15**, 630–638 (2017).

15. Minty, J. J. et al. Design and characterization of synthetic fungal-bacterial consortia for direct production of isobutanol from cellulosic biomass. Proceedings of the National Academy of Sciences **110**, 14592–14597 (2013).

16. Zuroff, T. R., Xiques, S. B. & Curtis, W. R. Consortia-mediated bioprocessing of cellulose to ethanol with a symbiotic clostridium phytofermentans/yeast co-culture. Biotechnology for biofuels **6**, 59 (2013).

17. Kato, S., Haruta, S., Cui, Z. J., Ishii, M. & Igarashi, Y. Stable coexistence of five bacterial strains as a cellulose-degrading community. Applied and Environmental Microbiology **71**, 7099–7106 (2005).

18. Liu, Y. et al. A three-species microbial consortium for power generation. Energy & Environmental Science **10**, 1600–1609 (2017).

19. Pham, V. H. & Kim, J. Cultivation of unculturable soil bacteria. Trends in Biotechnology **30**, 475–484 (2012).

20. Kaeberlein, T. Isolating "uncultivable" microorganisms in pure culture in a simulated natural environment. Science **296**, 1127–1129 (2002).

21. Moutinho, T. J. et al. Novel co-culture plate enables growth dynamic-based assessment of contact-independent microbial interactions. PLOS ONE **12**, e0182163 (2017).

22. Zhang, Z., Ji, H., Gong, G., Zhang, X. & Tan, T. Synergistic effects of oleaginous yeast rhodotorula glutinis and microalga chlorella vulgaris for enhancement of biomass and lipid yields. Bioresour Technol **164**, 93–9 (2014).

23. Abraham, W.-R. Applications and impacts of stable isotope probing for analysis of microbial interactions. Applied Microbiology and Biotechnology **98**, 4817–4828 (2014).

24. Wang, Y. et al. Reverse and multiple stable isotope probing to study bacterial metabolism and interactions at the single cell level. Analytical Chemistry **88**, 9443–9450 (2016).

25. Gebreselassie, N. A. & Antoniewicz, M. R. 13 c-metabolic flux analysis of co-cultures: A novel approach. Metabolic Engineering **31**, 132–139 (2015).

26. Zhang, C. et al. Ecological robustness of the gut microbiota in response to ingestion of transient food-borne microbes. The ISME Journal **10**, 2235–2245 (2016).

27. Medlock, G. L. et al. Inferring metabolic mechanisms of interaction within a defined gut microbiota. Cell Systems **7**, 245–257.e7 (2018).

28. Kim, T. Y., Sohn, S. B., Kim, Y. B., Kim, W. J. & Lee, S. Y. Recent advances in reconstruction and applications of genome-scale metabolic models. Current Opinion in Biotechnology **23**, 617–623 (2012).

29. Stolyar, S. et al. Metabolic modeling of a mutualistic microbial community. Mol Syst Biol **3**, 92 (2007).

30. Freilich, S. et al. Competitive and cooperative metabolic interactions in bacterial communities. Nature Communications **2**, 589 (2011).

31. Heinken, A., Sahoo, S., Fleming, R. M. T. & Thiele, I. Systems-level characterization of a host-microbe metabolic symbiosis in the mammalian gut. Gut Microbes **4**, 28–40 (2013).

32. Heinken, A. & Thiele, I. Systematic prediction of health-relevant human-microbial co-metabolism through a computational framework. Gut Microbes **6**, 120–130 (2015).

33. Heinken, A. & Thiele, I. Anoxic conditions promote species-specific mutualism between gut MicrobesIn silico. Applied and Environmental Microbiology **81**, 4049–4061 (2015).

34. Magnúsdóttir, S. et al. Generation of genome-scale metabolic reconstructions for 773 members of the human gut microbiota. Nature Biotechnology **35**, 81–89 (2016).

35. Zhuang, K. et al. Genome-scale dynamic modeling of the competition between rhodoferax and geobacter in anoxic subsurface environments. The ISME Journal **5**, 305–316 (2010).

36. Hanly, T. J. & Henson, M. A. Dynamic flux balance modeling of microbial co-cultures for efficient batch fermentation of glucose and xylose mixtures. Biotechnol Bioeng **108**, 376–85 (2011).

37. Gomez, J. A., Hffner, K. & Barton, P. I. DFBAlab: a fast and reliable MATLAB code for dynamic flux balance analysis. BMC Bioinformatics **15** (2014).

38. Harcombe, W. R. et al. Metabolic resource allocation in individual microbes determines ecosystem interactions and spatial dynamics. Cell Rep **7**, 1104–15 (2014).

39. Henson, M. A. & Phalak, P. Microbiota dysbiosis in inflammatory bowel diseases: in silico investigation of the oxygen hypothesis. BMC Systems Biology **11** (2017).

40. Henson, M. & Phalak, P. Byproduct cross feeding and community stability in an in silico biofilm model of the gut microbiome. Processes **5**, 13 (2017).

41. Bauer, E., Zimmermann, J., Baldini, F., Thiele, I. & Kaleta, C. BacArena: Individual-based metabolic modeling of heterogeneous microbes in complex communities. PLOS Computational Biology **13**, e1005544 (2017).

42. Chan, S. H., Friedman, E. S., Wu, G. D. & Maranas, C. D. Predicting the longitudinally and radially varying gut microbiota composition using multi-scale microbial metabolic modeling. Processes **7**, 394 (2019).

43. Zomorrodi, A. R. & Maranas, C. D. OptCom: A multi-level optimization framework for the metabolic modeling and analysis of microbial communities. PLoS Computational Biology **8**, e1002363 (2012).

44. Khandelwal, R. A., Olivier, B. G., Rling, W. F. M., Teusink, B. & Bruggeman, F. J. Community flux balance analysis for microbial consortia at balanced growth. PLoS ONE **8**, e64567 (2013).

45. Chan, S. H. J., Cai, J., Wang, L., Simons-Senftle, M. N. & Maranas, C. D. Standardizing biomass reactions and ensuring complete mass balance in genome-scale metabolic models. Bioinformatics **33**, 3603–3609 (2017).

46. Shoaie, S. et al. Quantifying diet-induced metabolic changes of the human gut microbiome. Cell Metab **22**, 320–31 (2015).

47. Henson, M. A. & Phalak, P. Suboptimal community growth mediated through metabolite crossfeeding promotes species diversity in the gut microbiota. PLOS Computational Biology **14**, e1006558 (2018).

48. Zelezniak, A. et al. Metabolic dependencies drive species co-occurrence in diverse microbial communities. Proc Natl Acad Sci U S A **112**, 6449–54 (2015).

49. Zomorrodi, A. R. & Segrè, D. Genome-driven evolutionary game theory helps understand the rise of metabolic interdependencies in microbial communities. Nature Communications **8** (2017).

50. Pacheco, A. R., Moel, M. & Segrè, D. Costless metabolic secretions as drivers of interspecies interactions in microbial ecosystems. Nature Communications **10** (2019).

51. Dubey, G. P. & Ben-Yehuda, S. Intercellular nanotubes mediate bacterial communication. Cell **144**, 590–600 (2011).

52. Pande, S. et al. Metabolic cross-feeding via intercellular nanotubes among bacteria. Nature Communications **6** (2015).

53. Bergstrom, C. T. & Lachmann, M. The red king effect: When the slowest runner wins the coevolutionary race. Proceedings of the National Academy of Sciences **100**, 593–598 (2003).

54. Blaser, M. J. & Kirschner, D. The equilibria that allow bacterial persistence in human hosts. Nature **449**, 843–849 (2007).

55. Gore, J., Youk, H. & van Oudenaarden, A. Snowdrift game dynamics and facultative cheating in yeast. Nature **459**, 253–256 (2009).

56. Frey, E. Evolutionary game theory: Theoretical concepts and applications to microbial communities. Physica A: Statistical Mechanics and its Applications **389**, 4265–4298 (2010).

57. Adami, C., Schossau, J. & Hintze, A. Evolution and stability of altruist strategies in microbial games. Physical Review E **85** (2012).

58. Kallus, Y., Miller, J. H. & Libby, E. Paradoxes in leaky microbial trade. Nature Communications **8** (2017).

59. Hummert, S. et al. Evolutionary game theory: cells as players. Mol. BioSyst. **10**, 3044–3065 (2014).

60. Schuster, S., Kreft, J.-U., Schroeter, A. & Pfeiffer, T. Use of game-theoretical methods in biochemistry and biophysics. Journal of Biological Physics **34**, 1–17 (2008).

61. Orth, J. D., Thiele, I. & Palsson, B. O. What is flux balance analysis? Nature Biotechnology **28**, 245–248 (2010).

62. Ferriere, R., Bronstein, J. L., Rinaldi, S., Law, R. & Gauduchon, M. Cheating and the evolutionary stability of mutualisms. Proceedings of the Royal Society of London. Series B: Biological Sciences **269**, 773–780 (2002).

63. Ferrière, R., Gauduchon, M. & Bronstein, J. L. Evolution and persistence of obligate mutualists and exploiters: competition for partners and evolutionary immunization. Ecology Letters **10**, 115–126 (2007).

64. Medaney, F., Dimitriu, T., Ellis, R. J. & Raymond, B. Live to cheat another day: bacterial dormancy facilitates the social exploitation of β-lactamases. The ISME Journal **10**, 778–787 (2015).

65. Waite, A. J. & Shou, W. Adaptation to a new environment allows cooperators to purge cheaters stochastically. Proceedings of the National Academy of Sciences **109**, 19079–19086 (2012).

66. Hom, E. F. Y. & Murray, A. W. Niche engineering demonstrates a latent capacity for fungal-algal mutualism. Science (2014).

67. Aung, H. W., Henry, S. A. & Walker, L. P. Revising the representation of fatty acid, glycerolipid, and glycerophospholipid metabolism in the consensus model of yeast metabolism. Industrial Biotechnology **9**, 215–228 (2013).

68. Imam, S. et al. A refined genome-scale reconstruction of chlamydomonas metabolism provides a platform for systems-level analyses. The Plant Journal **84**, 1239–1256 (2015).

69. Morris, J. J., Lenski, R. E. & Zinser, E. R. The black queen hypothesis: evolution of dependencies through adaptive gene loss. MBio **3**, e00036–12 (2012).

70. Chan, S. H. J., Simons, M. N. & Maranas, C. D. SteadyCom: Predicting microbial abundances while ensuring community stability. PLOS Computational Biology **13**, e1005539 (2017).

71. Liu, J., Ploskas, N. & Sahinidis, N. V. Tuning BARON using derivative-free optimization algorithms. Journal of Global Optimization (2018).

72. King, Z. A. et al. Escher: A web application for building, sharing, and embedding data-rich visualizations of biological pathways. PLOS Computational Biology **11**, e1004321 (2015).